Inhibitor Design for SARS Coronavirus Main Protease Based on "Distorted Key Theory"

Qi-Shi Du[1,2,*], Hao Sun[1] and Kuo-Chen Chou[2]

[1]*Tianjin Normal University, Institute of Bioinformatics and Drug Discovery, Tianjin, 300074, China;* [2]*Gordon Life Science Institute, 13784 Torrey Del Mar Drive, San Diego, California 92130, USA*

Abstract: In order to find effective peptide inhibitors against SARS CoV M^{pro}, an analysis was performed for 11 oligopeptides that can be cleaved by the SARS coronavirus main protease (CoV M^{pro}, or $3CL^{pro}$). Flexible molecular alignments of the 11 cleavable peptides have provided useful insights into the chemical properties of their amino acid residues close to the cleavage site. Moreover, it was found through the ligand-receptor docking studies that of the 11 cleavable peptides, NH_2-ATLQ↓AIAS-COOH and NH_2-ATLQ↓AENV-COOH had the highest affinity with SARS CoV M^{pro}. The two octapeptides were selected as initial templates for further chemical modification to make them become effective inhibitors against the SARS enzyme according to the "distorted key" theory [K. C. Chou, Analytical Biochemistry 233 (1996) 1-14]. The possible chemical modification methods are proposed and examined. The approach developed in this study and the findings thus obtained might stimulate new strategies and provide useful information for drug design against SARS.

Key Words: SARS, CoV M^{pro}, protease inhibitor, cleavable peptides, rack mechanism, Chou's distorted key theory, bioinformatics.

I. INTRODUCTION

Many evidences indicate that a previously unrecognized coronavirus exist in SARS (Severe Acute Respiratory Syndrome) patients. The newly-found virus, called SARS-coronavirus (SARS-CoV), is the culprit of SARS. It is also known that the process of cleaving the SARS-CoV polyproteins by a special proteinase, the so-called SARS coronavirus main proteinase (CoV M^{pro}), is a key step for the replication of SARS-CoV. The functional importance of the M^{pro} in the viral life cycle has made it an attractive target for developing drugs against SARS.

II. DISTORTED KEY THEORY AND CLEAVABLE PEPTIDES

One of the key initial steps for finding drugs against SARS is to search for cleavable peptides by the SARS CoV M^{pro} [1-6]. Many efforts have been made in the search for cleavable peptides by HIV protease in developing drugs for AIDS (Acquired Immune Deficiency Syndrome) therapy [7-14]. The relationship between the cleavable peptides by an enzyme and its inhibitors derived from these peptides is based on the "distorted key" theory, as originally elaborated by Chou [15]. A schematic illustration to show the application of the theory for finding inhibitors against SARS enzyme is given in Fig. **1**, where panel (a) corresponds to the state that a cleavable peptide is fittingly bound to the active site of SARS enzyme during the cleavage process and panel (b) reveals that although still tightly bound to the active site, the peptide lost its cleavability due to its scissile bond being modified from a conjugate π bond to a strong hybrid bond. Such a modified peptide can be linked to a distorted key, which can be inserted into a lock but can neither open the lock nor be pulled out from it, and hence automatically become a competitive inhibitor of the enzyme [16].

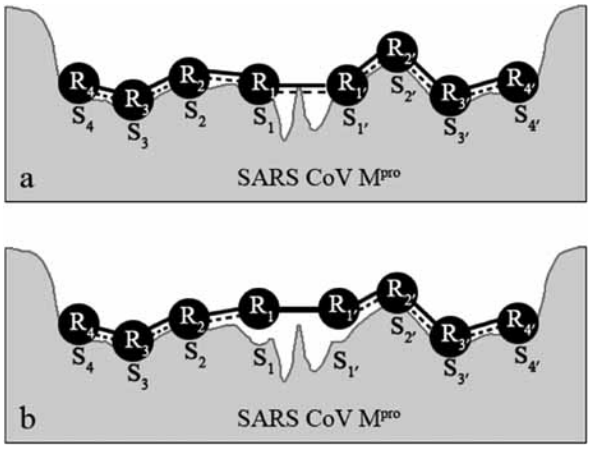

Fig. (1). Schematic illustration to show (a) a cleavable octapeptide is chemically effectively bound to the active site of SARS CoV M^{pro}, and (b) although still bound to the active site, the peptide lost its cleavability after its scissile bond is modified to a strong hybrid peptide bond. The eight residues of the peptide are sequentially symbolized by R_4, R_3, R_2, R_1, $R_{1'}$, $R_{2'}$, $R_{3'}$, and $R_{4'}$, and their counter parts by S_4, S_3, S_2, S_1, $S_{1'}$, $S_{2'}$, $S_{3'}$, and $S_{4'}$, respectively. Adapted from Fig. **2** of Chou [15] with permission.

By following the same procedure as described in [5], a total of 36 SARS coronaviruses were used for statistical analyses and 11 cleavage sites in polyprotein pp1ab detected. Listed in Table **1** are the 11 cleavage sites and the corresponding cleavable peptides. The arrow "↓" shows the cleavage sites [13,15]. Each of the 11 cleavable peptides consists

*Address correspondence to this author at the Gordon Life Science Institute, 13784 Torrey Del Mar Drive, San Diego, California 92130, USA; Tel: 086-22-2354-0997; Fax: 086-22-2354-0187; Email: lifescience@san.rr.com

1573-4064/07 $50.00+.00

Table 1. The 11 Cleavable Peptides Taken from Polyproteins pp1a and pp1ab of SARS CoV, TOR2 (NC_004718)[a]

No.	R6	R5	R4	R3	R2	R1		$R_{1'}$	$R_{2'}$	$R_{3'}$	$R_{4'}$	$R_{5'}$	$R_{6'}$	Length
P1	T	S	A	V	L	Q	↓	S	G	F	R	K	M	306
P2	S	G	V	T	F	Q	↓	G	K	F	K	K	I	290
P3	K	V	A	T	V	Q	↓	S	K	M	S	D	V	83
P4	N	R	**A**	**T**	**L**	**Q**	↓	**A**	I	A	S	E	F	198
P5	S	A	V	K	L	Q	↓	N	N	E	L	S	P	113
P6	A	T	V	R	L	Q	↓	A	G	N	A	T	E	139
P7	R	E	P	L	M	Q	↓	S	A	D	A	S	T	932
P8	P	H	T	V	L	Q	↓	A	V	G	A	C	V	601
P9	N	V	**A**	**T**	**L**	**Q**	↓	**A**	E	N	V	T	G	527
P10	T	F	T	R	L	Q	↓	S	L	E	N	V	A	346
P11	F	Y	P	K	L	Q	↓	A	S	Q	A	W	Q	298

[a]The arrow "↓" shows the cleavage sites. The 11 cleavable peptides consist of the amino acids on both sides of the cleavage sites.

of 12 amino acid residues with the cleavage site at the position between $R_1$and $R_{1'}$. According to the "rack mechanism" [17-19], these cleavable peptides must have strong binding affinity with SARS CoV M^{pro}, and hence can serve as a template reference for finding competitive inhibitors.

The statistical distribution of amino acid residues surrounding the cleavable peptide bond (R_1 - $R_{1'}$) was calculated, and the results are shown in the Fig. **2**. As shown from the figure, the position R_1 is invariably occupied by amino acid residue Gln. Amino acid residue Leu has the largest probability at position R_2, while for position $R_{1'}$, amino acid residues Ala and Ser have larger probabilities than others. On position R_4, amino acid residue Ala has the largest probability (36.4%) and on position R_3, amino acid residue Thr has the largest probability (36.4%). Table **2** lists the percentages of amino acid distribution around the cleavage sites of SARS CoV M^{pro} derived from the 36 SARS coronaviruses.

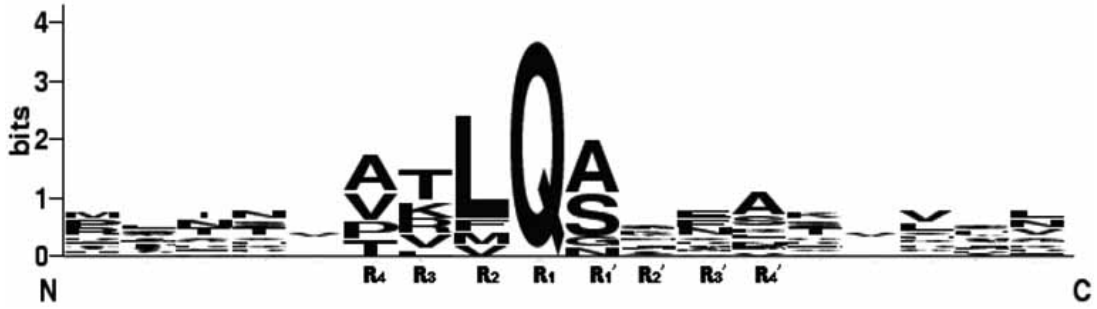

Fig. (2). The cleavage specificities of SARS-Coronaviruses. The statistical data are converted to logo presentations in which the size of an amino acid is proportional to its conservation at a specific position and the sampling size. The amino acid conservation is measured in bits of information plotted on a vertical axis whose upper limit is determined by the diversity of 20 natural amino acids expressed as a logarithm of 2 [32]. In the statistical calculation, the polyprotein pp1ab sequences of 36 SARS coronaviruses were used.

Table 2. The Percentage Probabilities of Amino Acids on the Cleavage Specific Positions of SARS CoV M^{pro}

Site	Frequent percentage of amino acids			
R_4	A：36.4%	V: 27.3%	P: 18.2%	T: 18.2%
R_3	T: 36.4%	K: 18.2%	R: 18.2%	V: 18.2%
R_2	L: 72.7%	F: 9.1%	M: 9.1%	V: 9.1%
R_1	Q：100%	---	---	---
$R_{1'}$	A: 45.5%	S: 36.4%	G: 9.1%	N: 9.1%

III. ALIGNMENT AND DOCKING

In order to find the physical and chemical properties of the amino acids from positions R_4 to $R_{4'}$, we aligned the 11 cleavable peptides. The results are given in Fig. **3**, where panel (a) shows the lipophilicity and hydrophilicity of amino acid side chains of the 11 cleavable peptides. The blue is used for the hydrophilic surfaces and the green for the lipophilic surfaces. As we can see, residues at R_2 and R_4 are the most lipophilic; residues at $R_{1'}$ and $R_{3'}$ are partially lipophilic residues. On the other hand, residues at R_1 are the most hydrophilic and residues at R_3 and R_4 are partially hydro-philic residues. The residues at $R_{2'}$ could be lipophilic or hydrophilic. Shown in (Fig. **3a**) are also the sizes of the side chains of amino acids. The size of side chain of $R_{1'}$ is very small, and the volumes of side chains of residues R_3, R_2 and $R_{3'}$ are larger than others. Aromatic groups are on the positions R_2 and $R_{3'}$. Shown in (Fig. **3b**) are the pharmacophore types of atoms in the relevant amino acid side chains. The colors used for pharmacophore types are as follows: white is for hydrogen bond donor; cyan for hydrogen bond acceptor; magenta for both acceptor and donor; light blue for cation or resonance cation; red for anion or resonance anion; dark green for hydrophobic atoms; and gray for other atoms. The residue R_2 is a purely lipophilic group. The residues at R_1 have hydrogen bond donor and cation, while those at R_3, $R_{2'}$, and $R_{4'}$ have both hydrogen bond donor and acceptor.

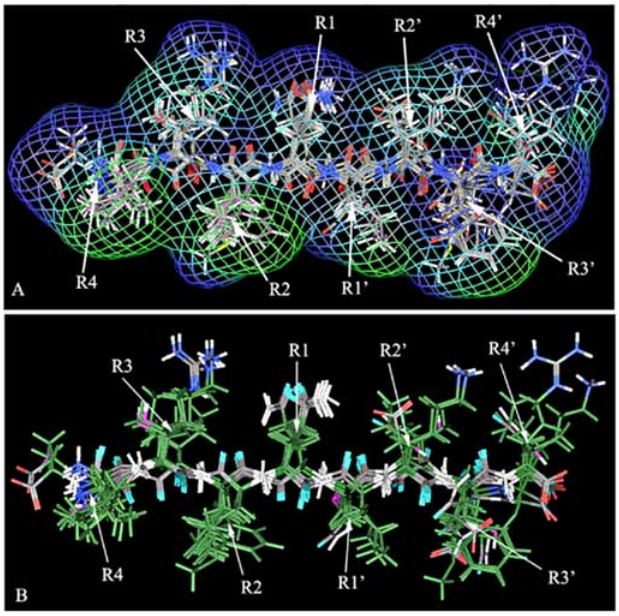

Fig. (3). The alignment of the 11 cleavable peptides. (a) Hydrophilic and hydrophobic surfaces of peptides. The green is for lipophilic regions and the blue is for hydrophilic regions. (b) Atomic pharmacophore types of peptides. Atoms are colored according to their pharmacophore type, donor is white, acceptor is cyan, acceptor and donor is magenta, cation or resonance cation is light blue, anion or resonance anion is red, hydrophobe is dark green, and gray is for other atoms. For interpretation of the references to color of the figure, the reader is referred to the web version of this paper.

The docking operations were performed for the 11 cleavable peptides with respect to SARS CoV M^{pro} by using the force field FFMM94. The amino acid residues of SARS CoV M^{pro} within 5Å [20-23] to the peptide were involved during the docking calculations. A total of 20 ligand-acceptor docking conformations were recorded and the docking conformation with the lowest docking energy was saved for every cleavable peptide. The summary of the docking calculations is given in Table **3**.

In the competitive interaction between the protease and ligands, the peptide with the lowest docking free energy will likely have the highest chance binding to the acceptor. As shown in Table **3**, the docking free energies of all the 11 cleavable peptides are in the same level. The peptide P9 has the lowest docking free energy and peptide P4 has the second lowest docking free energy. Therefore, peptides P9 and P4 may have higher binding affinity with SARS CoV main protease than the other cleavable peptides. The lower docking free energy of P9 and P4 can be explained according to the data in Tables **1** and **2**. It can be seen from Table **1** that the positions R_4, R_3, R_2, $R_1$and $R_{1'}$of peptides P9 and P4 are occupied by the amino acids A, T, L, Q, and A, as shown in bold letters; while from Table **2** we find that the five amino acids have the largest statistical probabilities on the positions R_4, R_3, R_2, $R_1$and $R_{1'}$. Therefore, of the 11 cleavable peptides, P9 and P4 are the best candidates for inhibitor design.

Shown in Fig. **4** is the docking conformation of peptide P9 with SARS CoV main protease. The SARS CoV M^{pro} is a dimer of protomers A and B [1,24]. Each protomer consists of three domains: domain I, II, and III. The protomers A and B combine at the domain III forming an angle a little less

Table 3. The Lowest Docking Free Energy of the 11 Cleavable Peptides with SARS CoV M^{pro}

Cleavable peptides	Energy/kJ	Cleavable peptides	Energy/kJ
P1	-3024.318	P7	-1146.233
P2	-2199.769	P8	-3072.839
P3	380.508	P9	-4072.685
P4	-3523.811	P10	-2958.428
P5	-2675.172	P11	-1688.867
P6	-2114.811		

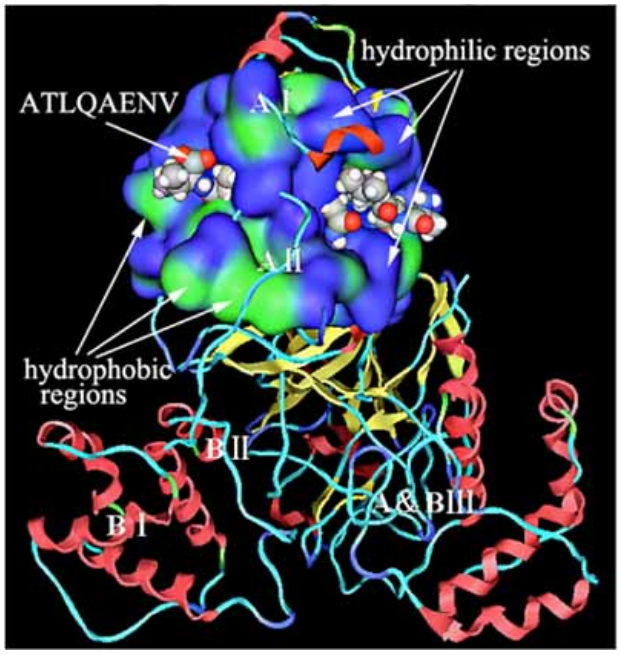

Fig. (4). The docking conformation of peptide P9 and SARS CoV M^{pro}. The green is for hydrophobic regions and the blue is for hydrophilic regions. The cleavable peptide P9 is shown as space filling model. The bioactive pocket is the cleavage cavity between domains I and II of protomer A. For interpretation of the references to color of the figure, the reader is referred to the web version of this paper.

than 90°. Only protomer A has bioactivity and the active site is in the cleavage cavity between domain I and domain II. The ball model of peptide P9 is shown in Fig. **4**, where the hydrophilic and hydrophobic surface of active pocket of SARS CoV M^{pro} is also displayed with green for the hydrophobic regions and the blue for the hydrophilic regions. Comparing Fig. **4** and (Fig. **3a**), we find a complimentary interaction between ligand and receptor: the hydrophilic parts of the ligand correspond to the hydrophilic regions of the receptor and the hydrophobic regions of the ligand correspond to the hydrophobic regions of the receptor. The cleavable peptide P9 is partially wrapped by protease, while the peptide bond to be cleaved is in the joining point between wrapped and exposed parts.

A close look at the docking conformation between P9 and the SARS CoV M^{pro} is given in Fig. **5**, where the peptide P9 is shown as the white stick model and the catalytic dyad His-41 and Cys-145 of the SARS CoV main protease shown as the ball-stick model. The peptide bond to be cleaved by the protease is colored green that is located between the catalytic dyad His-41 and Cys-145. There is a bridge water molecule near the catalytic dyad His-41 and Cys-145 and the peptide bond to be cleaved. The bridge water molecule joins the hydrolysis reaction and plays an important role [4,25] during the process.

IV. CHEMICAL MODIFICATION

Although a cleavable peptide can fittingly bind to the active site of a protease, it is not an inhibitor to the enzyme because it has a scissile peptide bond that will be eventually cleaved. However, a cleavable peptide can become an effective inhibitor after some proper chemical modification, as elaborated by Chou [15]. Converting the cleavable peptides to stable and bio-available drugs is a hot research topic in medicinal chemistry [2,3,15]. Here we present several possible chemical modification methods based on distorted key theory [15] and molecular modeling.

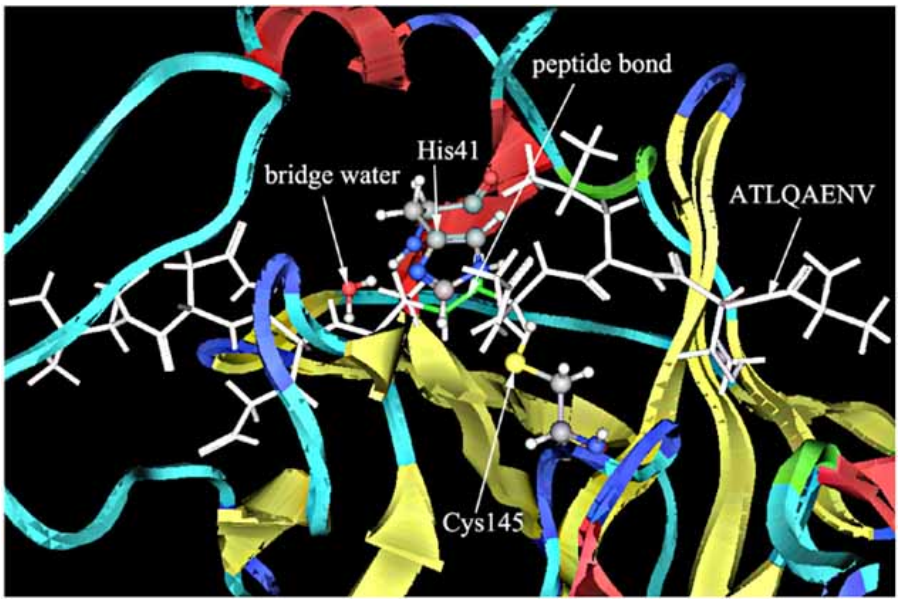

Fig. (5). A close look at the docking conformation of peptide P9 and SARS CoV M^{pro}. Cleavable peptide P9 is in the active pocket between domain I and II of SARS CoV M^{pro}. The peptide P9 is shown in white stick model. The peptide bond to be cleaved is shown in green. The cleavage dyad His-41 and Cys-145 of SARS CoV M^{pro} is shown as ball and stick model. A bridge water molecule is shown in figure near His-41. For interpretation of the references to color of the figure, the reader is referred to the web version of this paper.

The chemical modification is focused on the scissile peptide bond between $R_1$and $R_{1'}$that is to be cleaved by SARS CoV M^{pro}. According to the distorted key model, a cleavable oligo-peptide can automatically become a competitive inhibitor if its scissile peptide bond between $R_1$and $R_{1'}$ is replaced by a strong "hybrid peptide bond" (cf. Fig. **1**). In peptide P9, the positions $R_1$and $R_{1'}$ are occupied by amino acids Gln and Ala. The peptide bond CO ≃ NH between Gln and Ala is considered as a pseudo conjugate π-bond (here we use CO ≃ NH to emphasize the conjugate π-bond), which is easily hydrolyzed by SARS CoV M^{pro}. If the group CO is replaced by CH_2, or NH is replaced by CH_2, the conjugate π-bond will become a strong single bond, and hence the hydrolyzation will become very difficult [3,26,27]. In general, the methylamino isostere is prepared by the reduction of the amide bond with different reducing agents or by reductive amination of an amino aldehyde [28]. The isostere is incorporated into the ras farnesyl-protein transferase inhibitor that is a potential anticancer drug [29]. Pseudo peptide analogs containing reduced amide isostere are also shown to inhibit C_α-N-C cleavage in the gag region of HIV-1 protease [30].

Moreover, the possible chemical modifications for peptide P9 were also modeled by quantum chemical calculation. The ab initio HF/6-31G(d) was used to calculate the atomic charges of peptide P9. In the calculation, the SARS CoV M^{pro} and solvent water molecules were treated as background charges. The atomic charges on the two sides of the peptide bond before and after modification are summarized in Table **4**, in which the notations developed by Arno Spatola were adopted [31]. The symbol "Ψ[…]" denotes that the peptide bond is replaced by the atomic group in the bracket. It was observed that after CO was replaced by CH_2, the charge of the carbon atom in CH_2 turned to negative (-0.6572) from original a positive value (0.8612) in CO group, hence the nucleophilic attack by OH^- became impossible. Furthermore, the negative charge of N(NH) on the Ser side decreased to -0.2892 from -0.8190, and hence the electrophilic attack by H^+ became more difficult as well.

The effect of chemical modifications can also be examined by docking calculations. The docking free energies of peptide P9 and three modified peptide isosteres are shown in Table **5**, from which we can see that the docking free energies of peptide isosteres Ψ[CH_2NH], Ψ[CF_2NH] and Ψ[$COCF_2$] are lower than the docking free energy of P9. Among the three modified isosteres of peptide P9, Ψ[CH_2NH] has the lowest docking free energy. This result is fully consistent with the atomic charges shown in Table **4**, where Ψ[CH_2NH] has the most unfavorable atomic charges on atoms C(CO) and N(NH) for nucleophilic attack and electrophilic attack during the hydrolyzation reaction.

Table 5. The Docking Free Energy of Modified Peptide Isosteres

Modifications	Docking free energy (kJ/mol)
Peptide P9	-4072.685
GlnΨ[CH_2NH]Ala	-5117.230
GlnΨ[CF_2NH]Ala	-4849.055
GlnΨ[$COCF_2$]Ala	-4490.290

V. DISCUSSION AND CONCLUSION

According to the distorted key theory [13], the first step for protease inhibitor design is to find the cleavable peptides. In this study we searched the cleavable peptides by SARS CoV M^{pro} using the bioinformatics tools, and 11 cleavable peptides were found from the polyprotein pp1ab through genome annotation. Because such 11 peptides contain the original cleavage sites, they have high binding affinity with SARS CoV M^{pro}, as reflected by their predominant potentials in binding with the protease. Accordingly, these peptides are ideal starting templates for inhibitor design.

Chemical modification for the cleavable peptides was a follow-up step for making them become a real inhibitor. Useful information for inhibitor design was derived from these cleavable peptides through molecular modeling. It includes the size and lipophilicity of amino acid side chains, the hydrogen bond donors and acceptors, as well as the positions of cations and anions. The docking free energies of the 11 cleavable peptides with SARS CoV M^{pro} were computed.

Table 4. Atomic Charges in the Peptide Bond Gln—Ser Before and After Modifications

	Gln side-chain			Ser side-chain		
P9	**Cα**	**C(CO)**	**O(CO)**	**Cα**	**N(NH)**	**H(NH)**
–CO; NH–	0.0020	0.8612	-0.6219	0.3842	-0.8190	0.3497
Ψ[CH_2NH]	Cα	C(CH_2)	H(CH_2)	Cα	N(NH)	H(NH)
	0.0867	-0.6572	0.1251	-0.2121	-0.2892	0.1807
Ψ[CF_2NH]	Cα	C(CF_2)	F(CF_2)	Cα	N(NH)	H(NH)
	0.1182	0.3092	-0.0653	0.2597	-0.6483	0.3085
Ψ[$COCF_2$]	Cα	C(CO)	O(CO)	Cα	C (CH_2)	H(CH_2)
	0.0551	0.8437	-0.5940	0.4086	-0.6460	0.1511

The peptide with the smallest docking free energy was selected as a template for further chemical modification. According to the distorted key model (Fig. **1**), the chemical modification was focused on the peptide bond between $R_1$and $R_{1'}$. The peptide bond –CO ≃ NH– was replaced by "hybrid peptide bond" Ψ[CH_2NH]. The pseudopeptide analog thus obtained would resist the hydrolysis reaction catalyzed by protease, and hence be an effective inhibitor against SARS CoV M^{pro}. Such a chemical modification was supported by quantum chemical calculation and docking free energy.

Although the two octapeptides deduced in this paper have not been verified by experiments, it is quite encouraging to see that the octapeptide AVLQSGFR originally proposed by Chou *et al*. [1] through docking studies has been synthesized and tested [6]. The results indicate that the octapeptide AVLQSGFR is quite potent in inhibiting replication of the SARS coronavirus, and that no detectable toxicity was observed on Vero cells under the condition of experimental concentration.

REFERENCES

[1] Chou, K. C.; Wei, D. Q.; Zhong, W. Z. *Biochem. Biophys. Res. Commun.*, **2003**, *308*, 148.
[2] Chou, K. C. *Curr. Med. Chei.*, **2004**, *11*, 2105.
[3] Du, Q. S.; Wang, S. Q.; Wei, D. Q.; Zhu, Y.; Guo, H.; Sirois, S.; Chou, K. C. *Peptides*, **2004**, *25*, 1857.
[4] Du, Q. S.; Wang, S.; Wei, D. Q.; Sirois, S.; Chou, K. C. *Analyt. Biochem.*, **2005**, *337*, 262.
[5] Du, Q. S.; Wang, S. Q.; Jiang, Z. Q.; Gao, W. N.; Li, Y. D.; Wei, D. Q.; Chou, K. C. *Med. Chem.*, **2005**, *1*, 209.
[6] Gan, Y. R.; Huang, H.; Huang, Y. D.; Rao, C. M.; Zhao, Y.; Liu, J. S.; Wu, L.; Wei, D. Q. *Peptides*, **2006**, *27*, 622.
[7] Poorman, R. A.; Tomasselli, A. G.; Heinrikson, R. L.; Kezdy, F. J. *J. Biol. Chem.*, **1991**, *266*, 14554.
[8] Chou, K. C.; Zhang, C. T.; Kezdy, F. J. *Proteins: Struct., Funct., and Genet.*, **1993**, *16*, 195.
[9] Chou, K. C. *J. Biol. Chem.*, **1993**, *268*, 16938.
[10] Chou, J. J. *J. Prot. Chem.*, **1993**, *12*, 291.
[11] Chou, J. J. *Biopolymers*, **1993**, *33*, 1405.
[12] Thompson, T. B.; Chou, K. C.; Zheng, C. *J. Theor. Biol.* **1995**, *177*, 369.
[13] Chou, K. C.; Tomasselli, A. L.; Reardon, I. M.; Heinrikson, R. L. *Proteins: Struct., Funct., and Genet*, **1996**, *24*, 51.
[14] Cai, Y. D.; Chou, K. C. *Adv. in Engineering Software*, **1998**, *29*, 119.
[15] Chou, K. C. *Analyt. Biochem*, **1996**, *233*, 1.
[16] Chou, K. C.; Kezdy, F. J.; Reusser, F. *Analyt. Biochem.*, **1994**, *221*, 217.
[17] Chou, K. C.; Chen, N. Y.; Forsen, S. *Chemica Scripta*, **1981**, *18*, 126.
[18] Chou, K. C. *Biophys. Chem.*, **1988**, *30*, 3.
[19] Martel, P. *Prog. Biophys. Mol. Biol.*, **1992**, *57*, 129.
[20] Chou, K. C.; Watenpaugh, K. D.; Heinrikson, R. L. *Biochem. Biophys. Res. Commun*, **1999**, *259*, 420.
[21] Chou, K. C.; Tomasselli, A. G.; Heinrikson, R. L. *FEBS Letters*, **2000**, *470*, 249.
[22] Chou, K. C. *Biochem. Biophys. Res. Commun.*, **2004**, *319*, 433.
[23] Chou, K. C. *J. Proteome Res.*, **2004**, *3*, 1284.
[24] Yang, H.; Yang, M.; Ding, Y.; Liu, Y.; Lou, Z.; Zhou, Z.; Sun, L.; Mo, L.; Ye, S.; Pang, H.; Gao, G. F.; Anand, K.; Bartlam, M.; Hilgenfeld, R.; Rao, Z. *Proc. Natl. Acad Sci. USA*, **2003**, *100*, 13190.
[25] Chou, K. C.; Howe, W. J. *Biochem. Biophys. Res. Commun.*, **2002**, *292*, 702.
[26] Szelke, M.; Leckie, B. J.; Tree, M.; Brown, A.; Grant, J.; Hallett, A.; Hughes, M.; Jones, D. M.; Lever, A. F. *Hypertension*, **1982**, *4*, 59.
[27] Venkatesan, N., Kim, B. H. *Curr. Med. Chem.*, **2002**, *9*, 2243.
[28] Benkirane, N.; Guichard, G.; Briand, J. P.; Muller, S. *J. Biol. Chem.*, **1996**, *271*, 33218.
[29] Graham, S. L.; deSolms, S. J.; Giuliani, E. A.; Kohl, N. E.; Mosser, S. D.; Oliff, A. I.; Pompliano, D. L.; Rands, E.; Breslin, M. J.; Deana, A. A.; *et al*. *J. Med. Chem.*, **1994**, *37*, 725.
[30] Lowther, W. T.; Majer, P.; Dunn, B. M. *Protein Sci*, **1995**, *4*, 689.
[31] Spatola, A. F. In *Chemistry and Biochemistry of Amino Acids, Peptides and Proteins*; Weinstein, B., Ed.; Marcel Dekker: New York,, 1983; Vol. 7.
[32] Schneider, T. D.; Stephens, R. M. *Nucleic Acids Res.*, **1990**, *18*, 6097.

Received: 06 June, 2006 **Revised: 10 August, 2006** **Accepted: 11 August, 2006**